EvoDevo

RESEARCH

Open Access

Comparative Hox genes expression within the dimorphic annelid *Streblospio benedicti* reveals patterning variation during development

Jose Maria Aguilar-Camacho[1], Nathan D. Harry[1] and Christina Zakas[1*]

Abstract

Hox genes are transcriptional regulators that elicit cell positional identity along the anterior–posterior region of the body plan across different lineages of Metazoan. Comparison of Hox gene expression across distinct species reveals their evolutionary conservation; however, their gains and losses in different lineages can correlate with body plan modifications and morphological novelty. We compare the expression of 11 Hox genes found within *Streblospio benedicti,* a marine annelid that produces two types of offspring with distinct developmental and morphological features. For these two distinct larval types, we compare Hox gene expression through ontogeny using hybridization chain reaction (HCR) probes for in situ hybridization and RNA-seq data. We find that Hox gene expression patterning for both types is typically similar at equivalent developmental stages. However, some Hox genes have spatial or temporal differences between the larval types that are associated with morphological and life-history differences. This is the first comparison of developmental divergence in Hox gene expression within a single species and these changes reveal how body plan differences may arise in larval evolution.

Keywords Hox genes, Life-history, Marine larvae, Annelid development

Introduction

Hox genes are a classic example of conserved transcriptional regulators that assign positional identity along the anterior–posterior axis in all Metazoans [22, 34] at the cellular level [2, 55]. Therefore, they have received much attention when it comes to body plan evolution [2, 34]. While the conserved Hox gene expression pattern and synteny across distant taxa are renowned, there are many examples where changes in Hox gene expression have led to evolutionary diversification [29, 42]. However, the extent that Hox genes specifically contribute to developmental and morphological differences can be hard to disentangle because of the many phylogenetic and evolutionary differences that can arise [15, 37]. Here, we use an annelid with two distinct developmental pathways to compare how Hox gene expression shapes developmental and morphological differences.

In selected model organisms where Hox gene expression has been investigated, the genes appear in 'clusters' and are expressed in domains along the anterior–posterior axis at different developmental stages [15, 25, 51]. The expression patterns follow the same sequential order as their genome location, displaying spatial and temporal colinearity [11, 33].

There are, of course, exceptions to these rules. Hox genes are not always arranged in clusters; they may be on a single chromosome but spatially distinct (e.g., the

*Correspondence:
Christina Zakas
czakas@ncsu.edu
[1] Department of Biological Sciences, North Carolina State University, Raleigh, NC 27607, USA

mollusk *Crassostrea gigas* and the marine annelid worm *Capitella teleta*, which has a physically distant posterior Hox cluster in the genome [16, 31]. They could be in different chromosomes (e.g., in the spot octopus *Octopus binocularis* and the flatworm *Schmidtea mediterranea* [3, 10]). Also, Hox gene expression may deviate from spatial and temporal collinearity. For example, most of the Hox genes from the tunicate *Oikopleura dioica* are expressed in the tail and not in the anterior region at the larval stage; and in the brachiopod *Terebratalia transversa* Hox genes are not expressed collinearly at distinct developmental stages [42, 49, 50]. Hox genes may also take on different functions from the canonical expectation of specifying anterior–posterior segment identity. Hox genes can be co-opted or recruited to other functions that are lineage-specific (For Sprialian examples, *Post1* is expressed in the developing buccal lappets and in the developing light organ in the larva of the squid *Euprymna scolopes,* and this same orthologue is expressed in the swimming chaetal sacs in the Notochaete larva of the marine worm *Nereis virens* [28, 29].

To what extent do differences in Hox gene expression—in either time or space—lead to life-history and developmental changes? Studies of Hox gene expression patterns in annelids have shown a conserved expression pattern across related species, despite distinct larval life-histories [6, 16, 28]. However, Hox gene co-option is related to morphological novelties that are lineage-specific [6, 16, 28].

While many comparisons have been made across species, we take advantage of a model with an intraspecific developmental dimorphism to determine whether Hox gene expression differs based on development mode. This is essentially the opposite approach of comparing across distant lineages, instead looking at the closest possible evolutionary distance to identify the effects of subtle changes. Here we ask if Hox genes drive developmental divergence within a species. We use the estuarine annelid *Streblospio benedicti* that produces two types of offspring with distinct embryological and morphological features (reviewed in [56]). In this species, females brood embryos in a dorsal brood pouch before releasing them as swimming larvae. There are two types of females: They either produce many small eggs that develop as obligately feeding planktotrophic larvae, or a few large eggs that develop as non-feeding lecithotrophic larvae. Planktotrophic larvae spend 2–3 weeks feeding in the plankton before becoming competent to metamorphosis, while lecithotrophic larvae can settle to the benthos within a day of release. In addition to egg and larval size, there are distinct morphological differences between the swimming larval types. For example, planktotrophic larvae have swimming chaetae which are absent in the equivalent swimming lecithotrophic larvae (Fig. 1). Using this model, we compare Hox gene expression differences across divergent life-history modes while controlling for interspecific evolutionary differences. By determining Hox gene expression patterns at distinct developmental stages in the two developmental modes, we add to the growing understanding of annelid Hox gene evolution.

Results

Larval staging and developmental differences

The distinct larval and life-history dimorphism in *S. benedicti* is well characterized (reviewed in [19, 56]). While both larval morphs reach equivalent stages through unequal spiral cleavage, they differ in size and the absolute development time to each stage (Fig. 1). Despite this difference, the blastula, gastrula, and trochophore stages (where there is a distinct prototroch ciliary band and pear-shaped larva) are remarkably similar. Small planktotrophic larvae develop faster than their larger, yolky lecithotrophic counterparts (~8×difference by volume), which is expected as the larger cells take longer to divide [39].

We identified equivalent embryological and larval stages based on their conserved developmental patterns (Fig. 1). For this study, we investigated gastrula and trochophore stages for early gene expression. We termed the next stage as the '2-eye' stage. At this point, the larvae develop two red eyes simultaneously as the first anterior body segment of the trunk appears. Aside from size and yolk content, planktotrophic and lecithotrophic larvae appear similar at this stage.

Notable morphological differences arise at the '3-eye' stage. Larvae add an additional anterior-lateral eye on one side (usually the left) a day later. (While eye number is usually obvious, we also control our staging by development time, using larvae 24 h post 2-eye stage.) This is a long developmental stage where the larva grows by the addition of posterior segments. Larvae at this stage are 2–4 body segments long and the number of segments is indicative of larval age.

One major difference is that only the planktotrophic larvae grow 'swimming chaetae' which originate from paired, lateral chaetal sacs on the first body segments. The lecithotrophic offspring never produce these swimming chaetae, although they do have equivalent first chaetal sacs. Swimming chaetae or "provisional chaetae" are morphologically distinct from the smaller body chaetae found in the lateral, paired, parapodia of each segment.

The next developmental stage is when the larvae are typically released from the mother's brood pouch and most of the characteristic life-history differences occur. Larvae have four red eyes (two pairs) at this stage. These

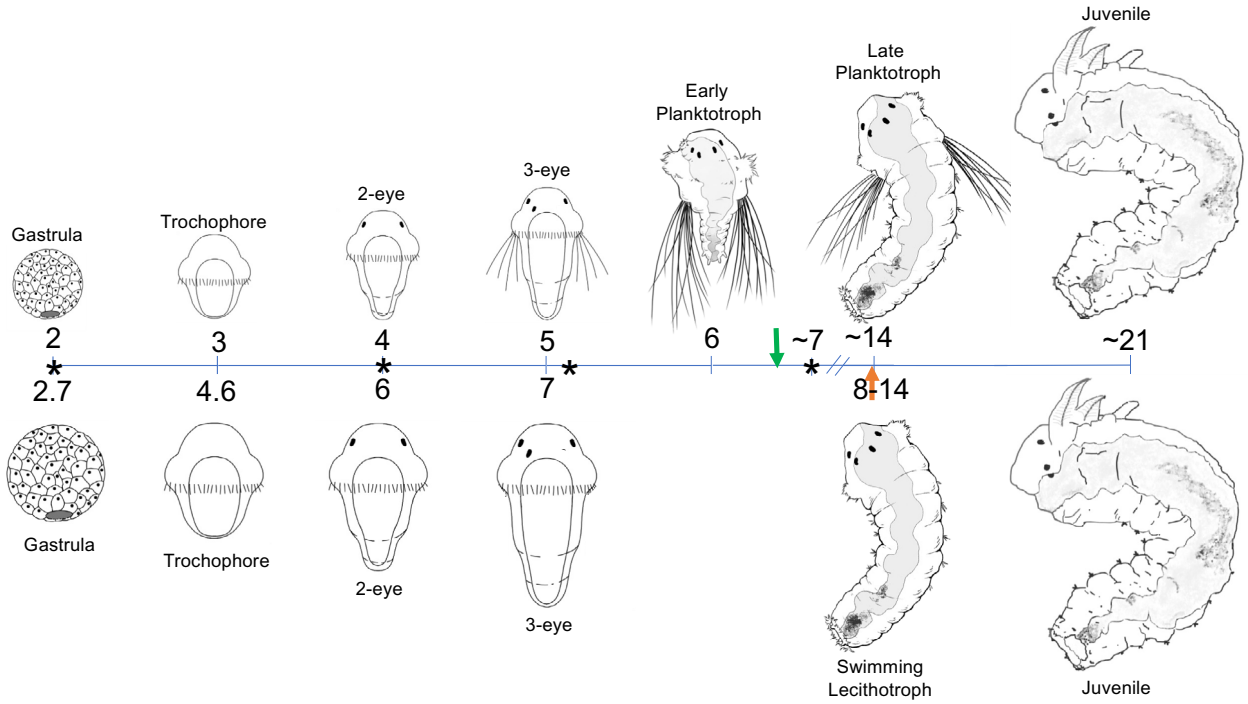

Fig. 1 Timeline of larval development in days post-fertilization. Both developmental types reach the same embryonic stages. Time is in days post-fertilization (dpf). Lecithotrophic embryos are delayed in developmental timing compared to planktotrophic larvae at the equivalent stage. Planktotrophic larvae have an extra swimming stage compared to the lecithotrophic larvae. Both types are morphologically indistinct by the early juvenile stage. Green and orange arrows indicate the approximate time when larvae are released from their mother. Asterisks indicate the RNAseq stages: gastrula, 2-eye, swimming larvae, and 1-week larvae

'early-planktotrophic' larvae can swim and ingest food as they have a functional mouth; a through-gut, a short trunk, and pronounced anal cirri on the tail. The swimming chaetae extend the full body length [46]. The 'late-planktotrophic' larval stage is approximately 10 days later, when the larvae have added additional posterior segments and feed, but they have not shed their swimming chaetae. We selected larvae that have ~ 12–13 segments for analysis, but planktotrophic larvae can take 2–4 weeks in the plankton at this stage before metamorphosing into juveniles. This 'late-planktotrophic' stage is morphologically like the 'swimming lecithotrophic' larval stage, with the notable exception of lecithotrophic larvae lacking swimming chaetae or pronounced anal cirri. The 'swimming lecithotrophic' larvae also have ~ 12–13 segments. Notably, the lecithotrophic larvae are released from their mother at this stage and only take ~ 1 day before metamorphosing. Therefore, females of each type brood their larvae for different periods of time: planktotrophic larvae are released at the early-planktotrophic stage around 7 days post-fertilization (dpf), while lecithotrophic larvae are released when they are competent to metamorphose, closer to 12–14 dpf. The time they spend as pelagic larvae is drastically different. However, at this late larval stage—just prior to metamorphosis—the two larval types are comparable in body plan and size. Both developmental types are sequentially adding segments to the posterior growth zone, and both appear competent to metamorphose.

At the 'juvenile stage', the two developmental modes converge in body plan and are morphologically indistinct. The juvenile has a peristomium and prostomium and a segmented body with ~ 13 segments (below the peristomium). One pair of palps and one pair of branchiae arise from the peristomium. In each segment, the notochaetae and neurochaetae are present. The late-planktotrophic larvae shed their swimming chaeta when undergoing metamorphosis to the early juvenile stage. It takes approximately 4 weeks for the early juvenile to become a reproductive adult [56].

Identification of the Hox genes

We identified 11 Hox genes in *S. benedicti* using a homologous gene approach: We assembled a transcriptome from RNAseq data of each developmental stage in the two developmental modes. We blasted known Hox genes from other spiralian species against our assembled transcriptome and genome to identify homologs in *S. benedicti*.

The 11 Hox genes are located on chromosome 7 of the *S. benedicti* genome, with an anterior cluster (*Lab, Pb, Hox3, Dfd, Scr, Lox5*, *Ant*, and *Lox4*) that spans ~ 463,000 kbp and a separate posterior cluster (*Lox2, Post2*, and *Post1*) further away on chromosome 7 [58],Fig. 2, Additional file 1: Table S3). We constructed the molecular phylogenetic tree of the Hox genes from aligned amino acid sequences across spiralian species. The 11 *S. benedicti* Hox genes are members of distinct clades containing other ortholog spiralian Hox genes (Fig. 3, Additional file 1: Fig. S1). This indicates that there are no duplication events for the Hox genes in the genome and gives high confidence that the Hox gene assignments are correct.

Hox gene expression patterns during development

To spatially and temporally visualize Hox gene expression, we developed probes for each of the 11 Hox genes using in situ hybridization chain reaction (HCR) [26]. To investigate body plan and developmental differences, we first identify the onset of Hox gene expression, as it could be different between the two developmental modes. At the gastrula and trochophore stage, no expression was detected for any of the 11 Hox genes in either developmental mode. The 2-eye stage is the earliest stage where we could visualize expression of any Hox gene (Figs. 4A, B, 5, 6). *Lab* is expressed in the ventral area in segments 2 and 3 in the late-planktotrophic larvae, swimming lecithotrophic larvae, and planktotrophic and lecithotrophic juvenile. *Lab* is expressed in the late-planktotrophic larvae and not in the early-planktotrophic larvae. *Pb* is expressed in the swimming chaetal sacs in the early-planktotrophic larvae and there is gene expression forming irregular circular spots in the latero/ventral part (segments 3–7) in the swimming lecithotrophic larvae (Fig. 4B, Additional file 1: Fig. S2). *Pb* has different expression patterns at the swimming larval stage (early-planktotrophic larvae and swimming lecithotrophic larvae) in the two developmental modes. *Pb* is expressed in the early-planktotrophic larvae and not in the late-planktotrophic larvae. *Hox3* is expressed at the posterior end in the 2-eye and 3-eye stages in the two developmental modes and in the posterior region in the early-planktotrophic larvae, in segments 8–13 in the swimming lecithotrophic larvae, late-planktotrophic larvae, planktotrophic juvenile, and lecithotrophic juvenile. *Dfd* is expressed in the mid-posterior region in the early-planktotrophic larvae and in segments 4–8 in the swimming lecithotrophic larvae. *Dfd* is expressed in the early-planktotrophic larvae and not in the late-planktotrophic larvae. *Scr* is expressed in the mid-posterior region in the early-planktotrophic larvae, in segments 4–8 in the swimming lecithotrophic larvae; in segments 4–9 in the late-planktotrophic, planktotrophic juvenile and lecithotrophic juvenile. *Lox5* is expressed in some segments of the posterior region in the 3-eye stage in the two developmental modes and in the early-planktotrophic larvae; in segments 8–12 in the late-planktotrophic larvae and in segments 5–11 in the swimming lecithotrophic larvae. *Ant* is expressed in one or two segments at the posterior region in the early-planktotrophic larvae; in segments 6–12 in the swimming lecithotrophic larvae; in segments 7–10 in the late-planktotrophic larvae, planktotrophic juvenile, and lecithotrophic juvenile. *Lox4* is expressed in segments 6–12 in the swimming lecithotrophic larvae, planktotrophic juvenile, and lecithotrophic juvenile. *Lox4* is expressed earlier in the lecithotrophic larvae than in the planktotrophic larvae. No expression was detected for *Post2* and *Lox2* at any stages in the two developmental modes (Fig. 4A, B). *Post1* in the planktotrophic larvae is first expressed as paired lateral spots in the chaetal sacs at the 2-eye stage. In the 3-eye stage, the larvae gain spots of lateral expression in each segment, which continues through the early-planktotophic stage. As late-planktotophic larvae, the expression in the chaetal sacs disappears, but the spotted lateral body segment expression remains through the juvenile stage. For lecithotrophic mode, the spotted lateral expression in the chaetal sacs does not appear until the 3-eye stage, concurrent with the lateral body segment spots. At the swimming lecithotrophic stage, the chaetal sac signal is lost, but the paired lateral segment spots remain (Figs. 4A, B, 5).

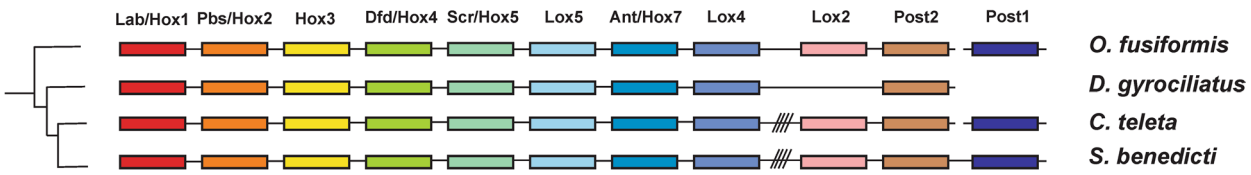

Fig. 2 Schematic representation of the Hox genes in *S. benedicti* and other polychaete species. Comparisons with *O. fusiformis* [37], *D. gyrociliatus* [36], and *C. teleta* [16]. Dashed lines indicate that the posterior Hox genes are physically separated from the anterior Hox genes forming split clusters in the genome

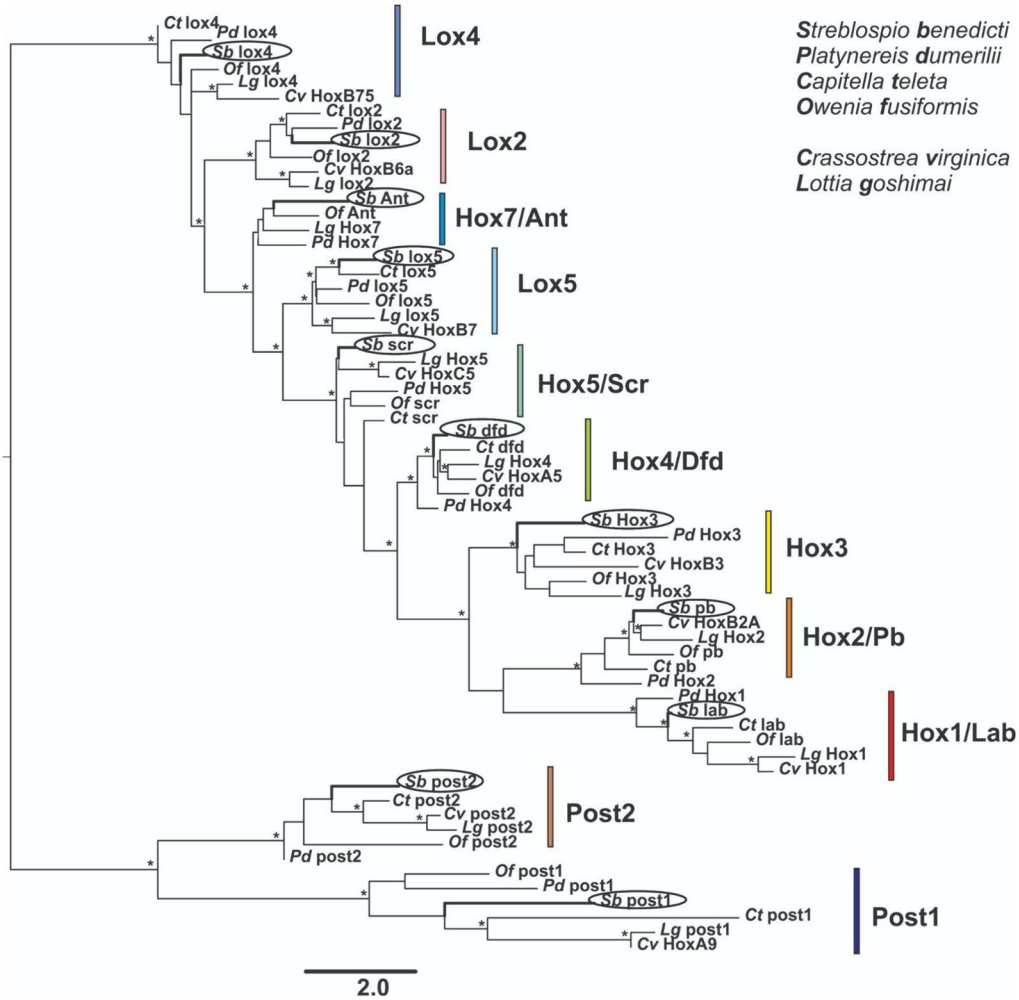

Fig. 3 Molecular phylogenetic tree of spiralian Hox genes and orthology assignment for S. benedicti Hox genes. Maximum-likelihood tree was calculated by three different methods: 1000 ultra-fast bootstrap replicates, 1000 replicates of the Shimodaira–Hasegawa approximate likelihood ratio test (SH-aLRT), and an approximate eBayes test. Asterisks above branches denote a support value of > 70% for all the three distinct molecular trees

Hox expression between the developmental morphs

Heterochronies (change in timing): Some Hox genes have a heterochronic shift in the timing of their expression. For *S. benedicti*, *Lox4* is expressed earlier in the swimming lecithotrophic larval stage than in the planktotrophic juvenile stage. However, it has the same relative expression pattern. *Post1* is expressed earlier in the 2-eye planktotrophic larval stage than in the 3-eye lecithotrophic larval stage (Figs. 4A, B, 6). *Dfd* and *Pb* stop being expressed one stage earlier in planktotrophic larvae (they disappear by the late-planktotrophic stage despite being present in the swimming lecithotrophic larvae).

Heterotopies (change in location): Pb is expressed in the swimming chaetal sacs in the early-planktotrophic larvae, but is only found in spots in the latero/ventral body segments in the swimming lecithotrophic larvae (Additional file 1: Fig. S2). *Post1* is also spatially different between the developmental types, appearing in the swimming chaetal sacs of the planktotrophic larvae for the first three stages, but only appearing in the lecithotrophic larvae swimming chaetal sacs at the 3-eye stage. However, the paired lateral expression of *Post1* in the body segments is expressed similarly across the two developmental modes (Figs. 4A, B, 5, 6).

RNA expression levels of the Hox genes

While we can visualize the onset and expression levels of the Hox genes using HCR in situ hybridization, we also wanted to compare Hox gene expression using a bulk RNAseq approach. We sequenced RNA from three developmental stages across both types: 16-cell,

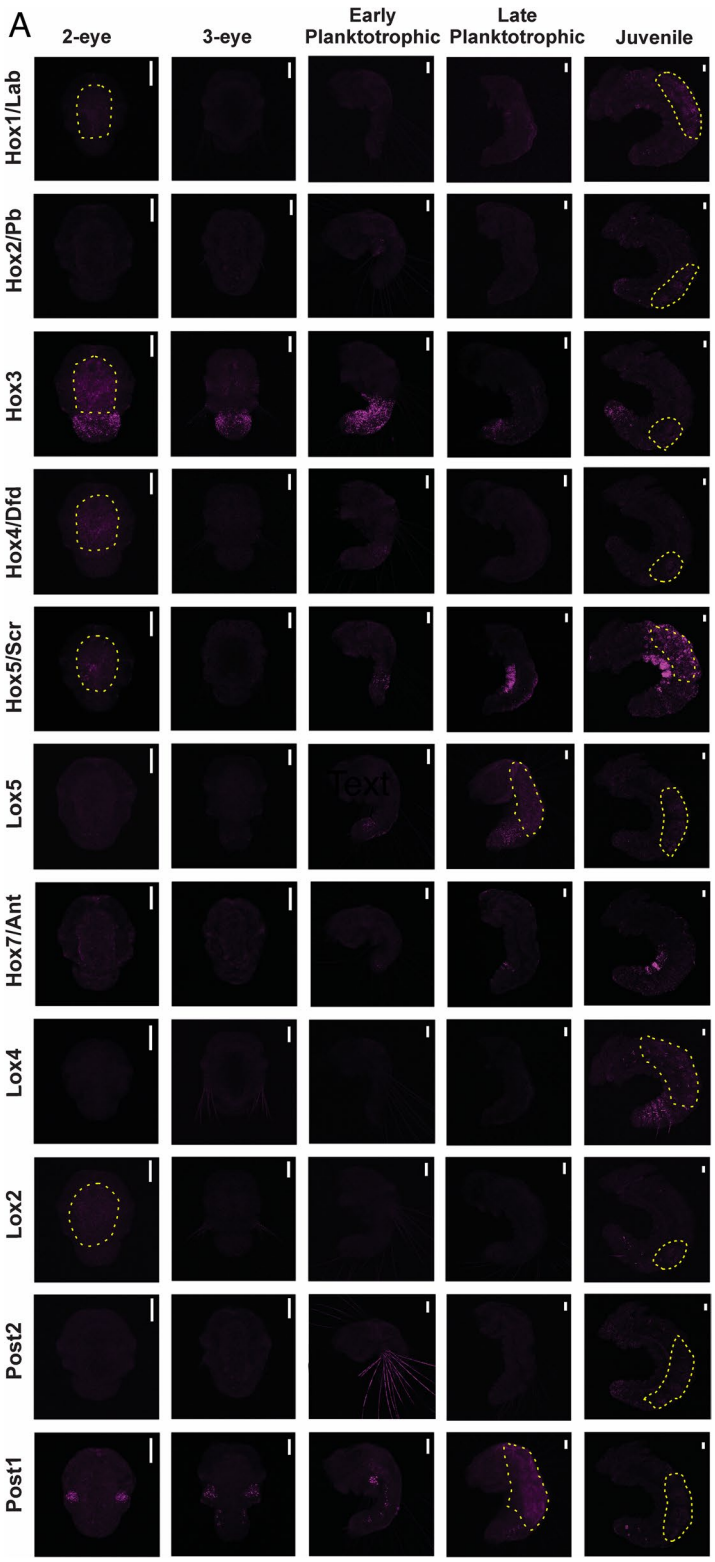

Fig. 4 **A** HCR in situ hybridization of the S. benedicti Hox genes at distinct developmental stages of the planktotrophic developmental mode. 2-eye and 3-eye stages are ventral view, and early planktotrophic, late planktotrophic, and juvenile are lateral view. Yellow dashed lines encircle confirmed autofluorescent regions. Scale bars = 50 µm. **B** HCR in situ hybridization of the S. benedicti Hox genes at distinct early developmental stages of the lecithotrophic developmental mode. 2-eye and 3-eye stages are ventral view, and early planktotrophic, late planktotrophic, and juvenile are lateral view. Yellow dashed lines encircle confirmed autofluorescent regions. Scale bars = 50 µm

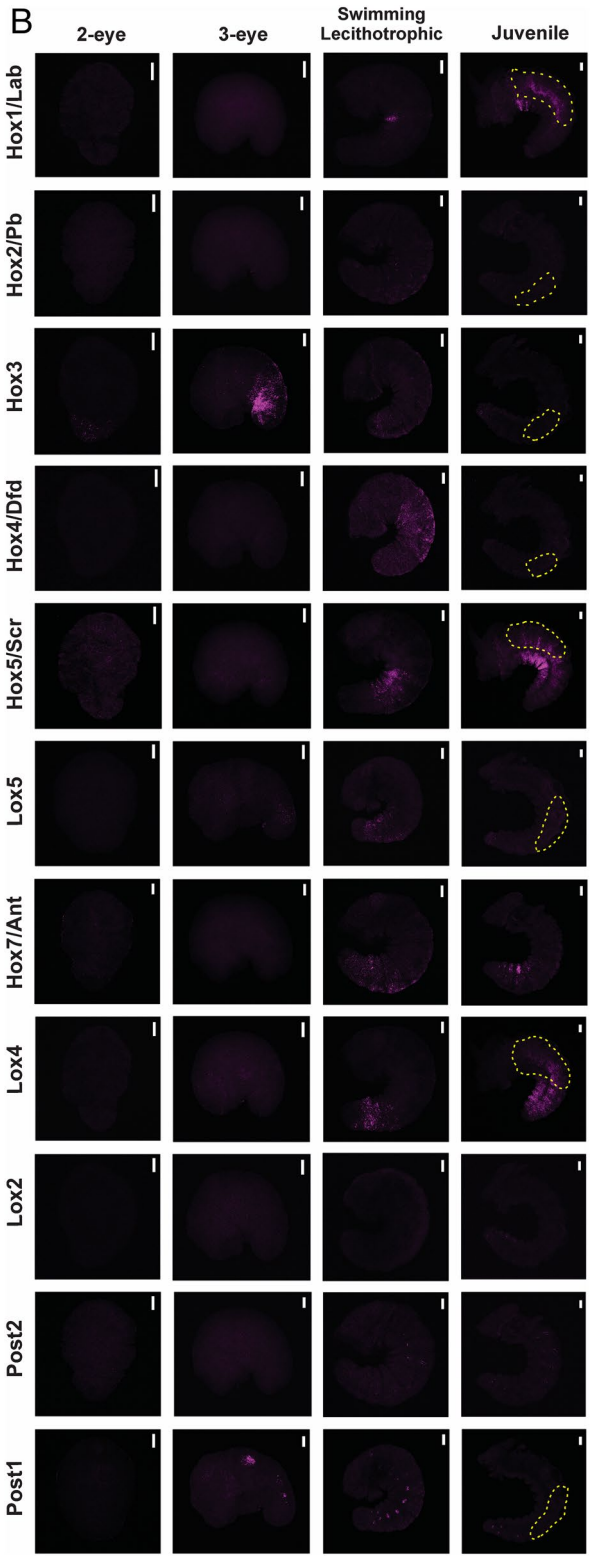

Fig. 4 continued

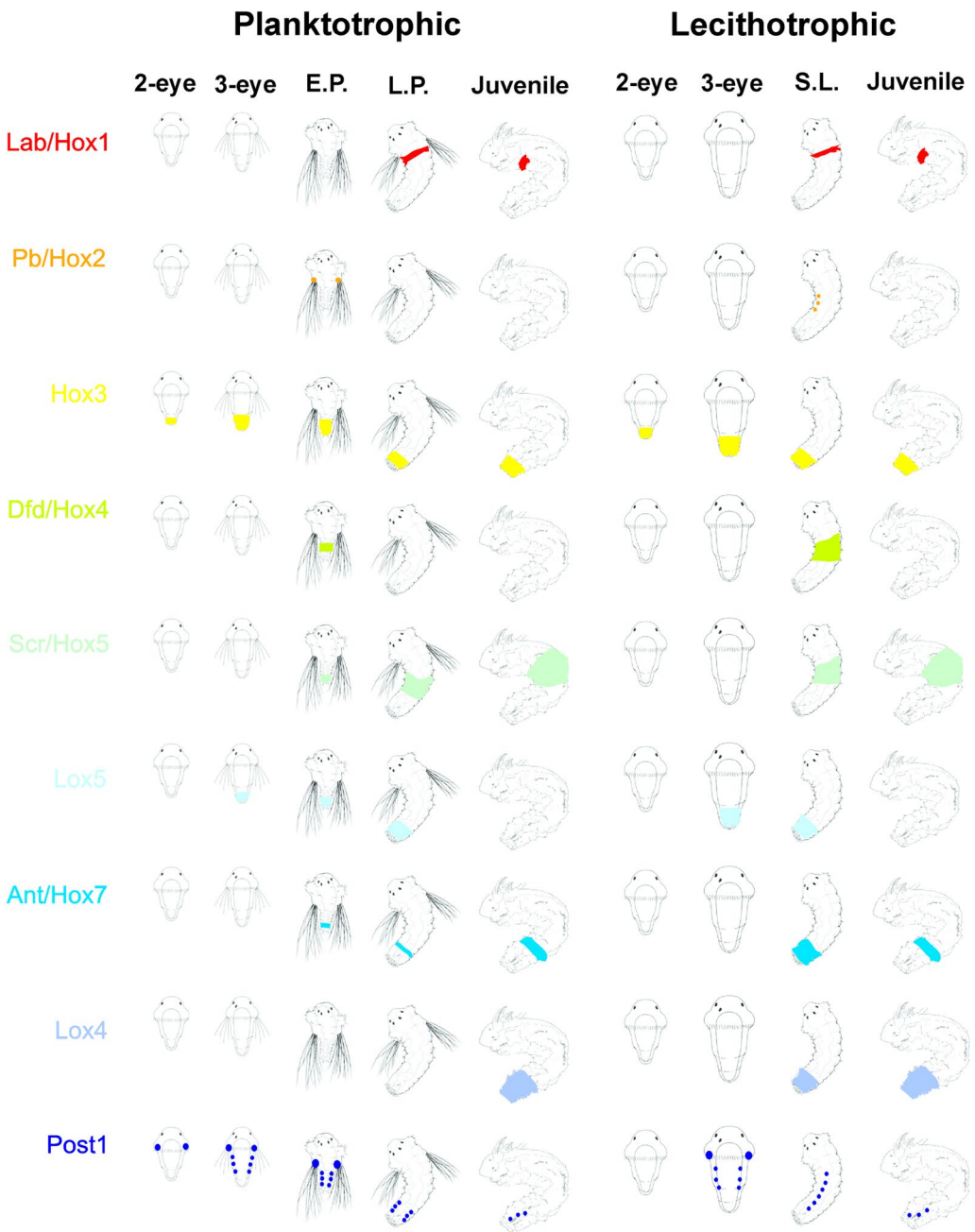

Fig. 5 Overview of the general Hox gene expression patterns at early life stages in the two developmental modes of S. benedicti. E.P. = early-planktotrophic, L.P. = late-planktotrophic, S.L. = Swimming Lecithotrophic. (In vivo Hox genes expression patterns are presented in Fig. 4.)

blastula, gastrula, 2-eye larvae, swimming larvae which are ~ 5–7 dpf (early-planktotrophic larvae and early swimming lecithotrophic larvae that we manually removed from the mother's brood pouch), and 1-week old larvae which are seven dpf ('late-planktotrophic' larvae and 'swimming lecithotrophic' larvae; [19]; Figs. 1, 7). We used RNAseq data both to identify Hox mRNAs for the HCR probe design and to quantify differential gene expression. We cannot detect any gene expression in these first three stages when using HCR, but we can compare the transcriptomic reads to the HCR patterns for the last three stages (Fig. 7). Although it is important to note that RNAseq and HCR are fundamentally different methodologies, and while patterns may be similar, we do not expect the results to directly translate across datasets. This result highlights why

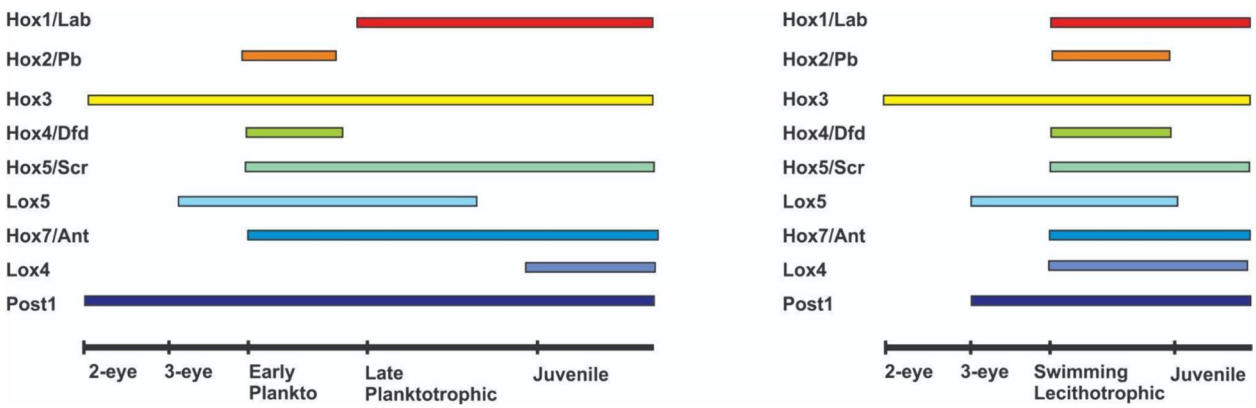

Fig. 6 Timing of Hox gene expression in the two developmental modes of S. benedicti. Planktotrophic developmental mode is left and lecithotrophic developmental mode is right

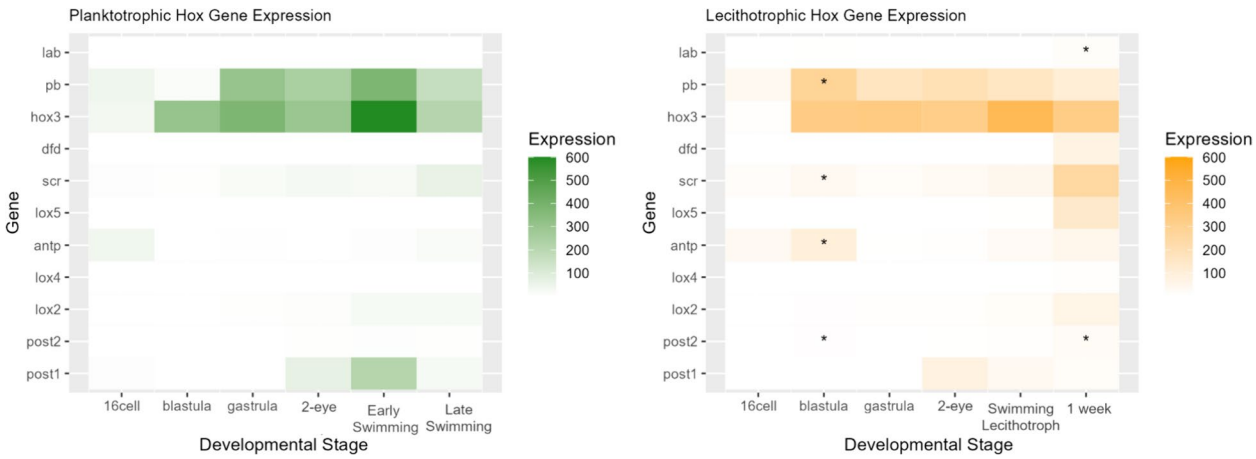

Fig. 7 Heatmap of RNAseq Hox gene expression. Number of reads mapped to each gene over development shows similarity in Hox gene expression patterns across the types. Asterisk indicates the gene is significantly differentially expressed at that time point compared to the other larval type as determined using DESeq2 and the full transcriptome dataset to assign significance. The six timepoints are equivalent stages across the two larval types. "1 week" larvae have not metamorphosed into juveniles and are late-stage swimming larvae

bulk RNAseq comparisons alone may not be sufficient to find spatial expression differences.

Overall Hox gene expression is quite low in the RNAseq dataset, but very similar between morphs. Some statistically significant differences in expression are indicated (based on the criteria for a minimum fold-change difference in expression greater than 2, and a $p < 0.05$ using the entire transcriptome with DEseq). Most significant differences in expression are at the blastula stage, with later stages having largely conserved Hox gene expression. This is consistent with other spiralian patterns of gene expression, where typically there is more divergence (across species) or variation (within species) in gene expression in early embryogenesis that converge around gastrulation [19, 37].

Discussion

This is the first comparison of developmental divergence in Hox genes expression within a species, which demonstrates the extent to which Hox genes can differ in larvae that make up alternate life-history modes. We see little evidence that the Hox genes drive developmental differences or are responsible for the divergence we see in overall larval morphology. Likely, the life-history differences and larval morphology arise from genes downstream of Hox expression in the developmental program.

S. benedicti Hox homolog conservation with other annelids

The 11 Hox genes we identified, and their order in the genome, are homologous to other spiralians, particularly other annelids [6, 14, 16, 23, 24, 31, 37, 47]. The

split anterior–posterior clustering occurs in other annelids, brachiopods, and mollusks [16, 37, 49]. The most closely related species where the Hox genes have been studied, the lecithotrophic annelid *Capitella teleta,* has a similar genomic organization and expression patterns in the swimming lecithotrophic larval type [16, 37]. In both *C. teleta* and *S. benedicti,* genes *Dfd* and *Lox5* are expressed in the mid and posterior region of the segmented body, while *Scr* in the mid region and *Lox4* in the posterior region [16].

Most bilaterians, including the annelids *C. teleta*, *O. fusiformis*, *A. virens*, *N. virens*, and *P. dumerilii,* generally follows the expected Hox pattern of spatial and temporal collinearity in expression over developmental time and segment addition [6, 28, 37]. In *S. benedicti*, we generally see the same pattern of spatial collinearity, with some exceptions noted below, but we do not see the same pattern of temporal collinearity.

Temporal disruption could be consistent with the need to maintain variable developmental programs in a single species. One explanation for the early expression of more 'anterior' Hox genes is secondary co-option of gene function. Canonical Hox gene function is the specification of anterior–posterior body segments, but non-canonical functions can arise leading to secondary expression patterns in different locations or times [15, 20, 49]. For example, temporal changes in both *S. benedicti* larvae compared to other bilaterians include early expression of *Hox3* and *Post1* (in both HCR and RNAseq data). *Post1* and *Pb* are expressed in the chaetal sacs leading to the possibility of earlier expression in these locations as a secondary co-option into a role in chaetogenesis. Similar atypical temporal patterns are also observed in some other annelids: *Hox3* is also expressed early in *C. teleta* (in RNAseq data; Martin-Zamora et al. [37]); In *P. duremilii, Pb* is expressed early at the internal zone of the swimming chaetal sacs in the late-trochophore stage [28], supporting that it may have a role in chaetal specification or initiation in annelids. *Post1* is expressed very early in *Nereis virens* based on in situ hybridization, and has a role in chaetogenesis [27, 28].

The spatial colinearity is generally what we expect for both larval types (Fig. 7). However, some genes are expressed in places that are not consistent with segment identity. For example, *Post1* and *Pb* are expressed in swimming chaetal sacs, which occurs in other annelids and brachiopods and indicates that it could be a spiralian-specific Hox role for the formation of body chaetae [27, 28, 49]. The disruption of spatial collinearity in the expression patterns of some Hox genes is observed in other spiralian species of annelids, mollusks, brachiopods, rotifers, and nemertean [15, 16, 20, 37, 48, 49].

No expression was detected for *Lox2* and *Post2* at any of the developmental stages of *S. benedicti*. *Post2* and *Lox2* have been reported as the most highly expressed Hox genes at the posterior end of the growing zone in the juveniles of other species of annelids such as: *C. teleta, P. dumerilli,* and *O. fusiformis* [16, 28, 37]. Further HCRs in the late juvenile stage from the two developmental modes should be undertaken to corroborate whether *Lox2* and *Post2* are expressed later at the posterior end of the growth zone.

Hox expression between the developmental morphs within *S. benedicti*

Despite the developmental and life-history differences between the larval modes, we see remarkably little differentiation between Hox gene expression in either the HCR or RNAseq datasets. For both developmental modes, the earliest Hox genes expression is at the 2-eye stage when the body segments just begin to arise. Most Hox genes turn on at stages when the segments are beginning to form (3-eye stage and swimming larval stage). The similarity in expression pattern between the larval types highlights that Hox gene expression, and more broadly its relationship to body plan specification and initiation, is not different between animals based on their trophic life-history mode. Rather, the differences in Hox timing we see across other spiralian species with alternate life-histories are likely due to larger phylogenetic and evolutionary differences.

While the majority of Hox gene expression is similar between the two developmental modes, there are some key differences. Notably, there are heterotopic and heteromorphic changes in some Hox gene expression. Heterotopic differences in expression occur in *Pb* and *Post1,* which may have been secondarily co-opted in planktotrophic larvae to regulate swimming chaetae formation between the two developmental modes. Heterochronies across species are difficult to detect due to the methodological barriers of assigning equivalent stages across divergent species. Changes in the relative timing of expression could lead to segment specification differences and drive morphological change across lineages [12, 44]. In *S. benedicti*, we see clear patterns of heterochrony in Hox gene expression across the types at relative stages (*Lox4* and *Post1*), indicating that changes in the regulatory timing may be easily evolved. However, it is unlikely that the heterochronic shifts we see in two Hox genes are a major driver of body plan and life-history diversification within *S. benedicti*, although they could contribute to specific morphological differences between the two types like the formation of swimming chaetae.

Despite being a single species, assigning equivalent stages within *S. benedicti* is also difficult at some stages.

Early embryological timepoints are clearly morphologically equivalent, but the larval stages are more difficult to compare. For example, the stage of larval release ('early-planktotrophic' larvae and 'swimming lecithotrophic' larvae) is equivalent stages in terms of many life-history traits. However, morphologically the 'swimming lecithotrophic' larvae are more similar to the 'late-planktotrophic' stage. Our Hox gene analysis clearly demonstrates that in terms of body plan formation, the former stages ('early-planktotrophic' larvae and 'swimming lecithotrophic' larvae) are the most equivalent despite the size and morphological differences. We have also recently completed an extensive gene expression analysis over larval development of the two morphs [19], which confirms that these are equivalent stages. Because the planktotrophic larvae have a longer and more differentiated larval phase covering two time points, where the lecithotrophic larvae have one, it leads to destinations of minor heterochronies. Namely, it is this staging difference that highlights the slightly different timing of *Lab*, *Pb*, and *Dfd* between the morphs.

When addressing heterochronies, it is critical to note that we are comparing the timing of gene expression at equivalent stages that differ in absolute time. In this way, the small number of heterochronic shifts we see are more surprising: consider that to have gene activation at the same relative time in development, the lecithotrophic offspring must initiate expression later in real time with a larger embryo (and cell) size than the planktotrophic larvae. The mechanisms that keep the same relative timing of expression in embryos of different sizes and ages are unknown. One theory of gene expression regulation in early embryos involves the nucleocytoplasmic (N:C) ratio (the proportion of cytoplasm to nuclear volume mediates transcriptional timing; [54]. However, this same N:C ratio would occur at different times in the two developmental types. Absolute time, or maternal timing, is also a key regulator in terms of transcript degradation or molecular half-lives [7, 30], maternal (or zygotic transcript degradation may occur at a different stage in the planktotrophic larvae compared to the lecithotrophic larvae. Again, a simple increase in egg size in the lecithotrophic type is not necessarily sufficient to explain the differences and similarities we see between the two developmental types.

Hox genes in *S. benedicti* are not a major contributor to morphological and life-history differences at the level of body plan. While overall patterns of Hox gene timing and location are quite similar in both types in the HCR and RNAseq data, there are multiple instances where Hox genes can be contributing to key life-history differences: some Hox genes (*Pb* and *Post1*) are clearly expressed differently in chaetal sacs and could have undergone a secondary co-option to regulate the formation of swimming chaetae in planktotrophic larvae. There are few heterochronic shifts in expression between the equivalent stages of the two developmental morphs, but whether these changes initiate any significant timing of downstream developmental differences remains to be determined.

Materials and methods

Identification of the Hox genes in the genome and transcriptome

RNAseq reads from six developmental stages [19] of both planktotrophic and lecithotrophic offspring were assembled with long-read (iso-seq CCS reads) guidance using the Trinity assembler [18]. Hox gene transcripts were identified from the resulting contigs using tblastn (e-value cutoff 1*10^-30) from the BLAST command line tools [4] and a set of Hox gene queries taken from other related taxa/species (Additional file 1: DataSheet). The 11 different contigs corresponding to 11 paralog genes are located in the genome of *S. benedicti* [58] using JBrowse [52]. The genomic location and gene length for each Hox gene is characterized in Additional file 1: Table S3.

Molecular phylogenetic analyses

We used Hox genes of other spiralian species from Genbank: *Platynereis dumerilii* [27, 38], *Capitella teleta* [16], *Owenia fusiformis* [37], *Crassostrea virginica* [41], and *Lottia goshimai* [21] to construct a gene phylogeny (Additional file 1: Table S2, Additional file 1: Data1). Amino acid sequences were aligned using MUSCLE which is included in the SEAVIEW software [13, 17]. A conservative alignment strategy was employed where all the positions that were spuriously aligned were excluded. The final alignment contains 64 sequences with 264 amino acid sites (Additional file 1: Data 2). Maximum-likelihood phylogenetic trees were constructed using the IQ-Tree software [43]. VT + I + G4 + F was the best-fit evolutionary model and -28796.8292 was the optimal log likelihood. Support values of the ML tree were calculated by three different methods: 1000 ultra-fast bootstrap replicates [40], 1000 replicates of the Shimodaira–Hasegawa approximate likelihood ratio test (SH-aLRT), and an approximate eBayes test [5] (Fig. 3, Additional file 1: Fig. S1).

Animal culturing

We collected embryos and larvae at each stage from lab reared animals of each developmental type as in Zakas [56]. Lecithotrophic worms were collected from Long Beach (California) and planktotrophic worms from Newark Bay (New Jersey [57]).

Hybridization chain reaction (HCR)

Multiplex probes of the 11 Hox gene transcripts of *S. benedicti* were designed using the HCR3.0 Probe Maker [26] (Additional file 1: Table S1). Exact oligo sequences and the associated hairpins are listed in the Additional file 1: DataSheet. The sequences generated by the software were used to order different batched DNA oligo pools (50 pmol DNA Pools Oligo Pool) from Integrated DNA Technologies, and resuspended to 1 pmol/µl in Nuclease Free Water. Different developmental stages from the two modes of *S. benedicti* were fixed in 4% paraformaldehyde at 4 °C overnight, transferred stepwise into 100% methanol, and kept at − 20 °C. Samples were rehydrated through a methanol/DEPC-treated PBSt series. Probe hybridization buffer, probe wash buffer, amplification buffers, and a DNA HCR amplifier hairpin set were purchased from Molecular Instruments. HCR was performed as previously described [9, 26].

Imaging

HCR samples were mounted in Slowfade Glass with DAPI and kept at 4 °C until imaging and imaged using Zeiss Laser Scanning Confocal Microscope LSM 710. Z-stack images (32 layers) were processed in ImageJ [1]. HCR probes were multiplexed, so that imaging a single individual would capture expression for 2–3 Hox genes (Additional file 1: Table S1). For each gene, larval stage, and larval type, we imaged two-to-five individuals to corroborate that the gene expression patterns. Four independent clutches of larvae were used for each set of multiplexed probes. Gene expression was considered real (and not background fluorescence) when a region only showed expression under one of the three possible color channels with distinct fluorescent spectra (Additional file 1: Table S1). Fluorescence that occurred in multiple channels and the controls was considered autofluorescence. In addition, samples from different Hox genes that have the same channel (same hairpins) were compared to identify any background signal (Additional file 1: Figs. S3 and S4). Control animals with only hairpins and no probes were also used to determine regions with background fluorescence. Chitinous regions of the larvae autofluorescence in some channels (mainly the green wavelength 488; as in the swimming chaeate of Fig. 4A early-planktotrophic larvae *Post2).*

RNA-seq data

Hox gene expression data were generated using RNAseq [19]. Each developmental stage consisted of three-to-five biological replicates of pooled whole embryos. Raw RNAseq reads were quality trimmed using FastP [8] and TrimGalore (cutadapt) [35] and then mapped to a reference transcriptome using Salmon [45]. The reference transcriptome was assembled using RNAseq reads and previously published IsoSeq data [58] in conjunction with the Trinity assembler [18] and assembled transcripts derived from Hox genes were identified using BLAST [4]. Sample expression quantification estimates were then normalized and statistical tests for differential expression between morphs at each stage were performed using the standard DESeq [32] workflow for time-series experiments in R. Heatmaps were made in R using the ggplot2 package [53].

Supplementary Information

The online version contains supplementary material available at https://doi.org/10.1186/s13227-024-00231-5.

Additional file 1.

Additional file 2.

Additional file 3.

Additional file 4.

Acknowledgements

Kayleigh McHugh helped with animal collection, maintenance, and fixation of samples. Mariusz Zareba assisted with the confocal analysis. Duygu Özpolat, Bria Metzger, Emma Kelley, and Veronica Acosta assisted with troubleshooting HCR *in situs*, and Ryan Null developed the probe finder for constructing HCR probes. Bruno Pernet, Carrie Albertin, and Matthew Rockman provided comments on the manuscript.

Author contributions

JMAC and CZ conceived, designed the work, and wrote the manuscript; JMAC did the HCR acquisition, analysis, and interpretation of data. NDH did the RNAseq acquisition, analysis, and interpretation of data. All authors reviewed the manuscript.

Funding

The initial work was completed at the Marine Biological Labs, Woods Hole MA with a Whitman Fellowship granted to. Zakas. The work of C. Zakas is supported by the NIH MIGMS under Grant No. 5R35GM142853.

Data availability

RNA reads are available at NCBI under BioProject PRJNA1008044.

Declarations

Competing interests

The authors declare no competing interests.

Received: 10 September 2024 Accepted: 12 September 2024
Published online: 27 September 2024

References

1. Abràmoff MD, Magalhães PJ, Ram SJ. Image processing with ImageJ. Biophotonics Int. 2004;11:36–42.
2. Afzal Z, Krumlauf R. Transcriptional regulation and implications for controlling hox gene expression. J Dev Biol. 2022;10:4.
3. Albertin CB, Simakov O, Mitros T, Wang ZY, Pungor JR, Edsinger-Gonzales E, Brenner S, Ragsdale CW, Rokhsar DS. The octopus genome and the

evolution of cephalopod neural and morphological novelties. Nature. 2015;524:220–4.
4. Altschul SF, Gish W, Miller W, Myers EW, Lipman DJ. Basic local alignment search tool. J Mol Biol. 1990;215:403–10.
5. Anisimova M, Gil M, Dufayard JF, Dessimoz C, Gascuel O. Survey of branch support methods demonstrates accuracy, power, and robustness of fast likelihood-based approximation schemes. Syst Biol. 2011;60:685–99.
6. Bakalenko NI, Novikova EL, Nesterenko AY, Kulakova MA. Hox gene expression during postlarval development of the polychaete *Alitta virens*. EvoDevo. 2013;4:1–17.
7. Buccitelli C, Selbach M. mRNAs, proteins and the emerging principles of gene expression control. Nat Rev Genet. 2020;21:630–44.
8. Chen S, Zhou Y, Chen Y, Gu J. Fastp: an ultra-fast all-in-one FASTQ preprocessor. Bioinform. 2018;34:i884–90.
9. Choi HM, Schwarzkopf M, Fornace ME, Acharya A, Artavanis G, Stegmaier J, Cunha A, Pierce NA. Third-generation in situ hybridization chain reaction: multiplexed, quantitative, sensitive, versatile, robust. Development. 2018;145:dev165753.
10. Currie KW, Brown DD, Zhu S, Xu C, Voisin V, Bader GD, Pearson BJ. HOX gene complement and expression in the planarian *Schmidtea mediterranea*. EvoDevo. 2016;7:1–11.
11. Denans N, Iimura T, Pourquié O. Hox genes control vertebrate body elongation by collinear Wnt repression. Elife. 2015;4:e04379.
12. Dobreva MP, Camacho J, Abzhanov A. Time to synchronize our clocks: connecting developmental mechanisms and evolutionary consequences of heterochrony. J Exp Zool B Mol Dev Evol. 2022;338:87–106.
13. Edgar RC. MUSCLE: a multiple sequence alignment method with reduced time and space complexity. BMC Bioinform. 2004;5:1–19.
14. Endo M, Sakai C, Shimizu T. Embryonic expression patterns of Hox genes in the oligochaete annelid *Tubifex tubifex*. Gene Expr Patterns. 2016;22:1–14.
15. Fröbius AC, Funch P. Rotiferan Hox genes give new insights into the evolution of metazoan body plans. Nat Commun. 2017;8:9.
16. Fröbius AC, Matus DQ, Seaver EC. Genomic organization and expression demonstrate spatial and temporal Hox gene colinearity in the lophotrochozoan *Capitella* sp. I PloS one. 2008;3:e4004.
17. Gouy M, Guindon S, Gascuel O. SeaView version 4: a multiplatform graphical user interface for sequence alignment and phylogenetic tree building. Mol Biol Evol. 2010;27:221–4.
18. Grabherr MG, Haas BJ, Yassour M, Levin JZ, Thompson DA, Amit I, Adiconis X, Fan L, Raychowdhury R, Zeng Q, Chen Z, Mauceli E, Hacohen N, Gnirke A, Rhind N, di Palma F, Birren BW, Nusbaum C, Linblad-Toh K, Friedman N, Regev A. Full-length transcriptome assembly from RNA-Seq data without a reference genome. Nat Biotechnol. 2011;29:644–52.
19. Harry ND, Zakas C. The role of heterochronic gene expression and regulatory architecture in early developmental divergence. Elife. 2024;13:RP93062.
20. Hiebert LS, Maslakova SA. Hox genes pattern the anterior-posterior axis of the juvenile but not the larva in a maximally indirect developing invertebrate, *Micrura alaskensis* (Nemertea). BMC Biol. 2015;13:1–12.
21. Huan P, Wang Q, Tan S, Liu B. Dorsoventral decoupling of Hox gene expression underpins the diversification of molluscs. Proc Natl Acad Sci USA. 2020;117:503–12.
22. Hombría JCG, García-Ferrés M, Sánchez-Higueras C. Anterior Hox genes and the process of cephalization. Front Cell Dev Biol. 2021;9:718175.
23. Irvine SQ, Martindale MQ. Expression patterns of anterior Hox genes in the polychaete *Chaetopterus*: correlation with morphological boundaries. Dev Biol. 2000;217:333–51.
24. Kourakis MJ, Martindale MQ. Hox gene duplication and deployment in the annelid leech *Helobdella*. Evol Dev. 2001;3:145–53.
25. Krumlauf R. Hox genes, clusters and collinearity. Int J Dev Biol. 2018;62:659–63.
26. Kuehn E, Clausen DS, Null RW, Metzger BM, Willis AD, Özpolat BD. Segment number threshold determines juvenile onset of germline cluster expansion in *Platynereis dumerilii*. J Exp Zool B Mol Dev Evol. 2022;338:225–40.
27. Kulakova MA, Kostyuchenko RP, Andreeva TF, Dondua AK. The Abdominal-B-like gene expression during larval development of *Nereis virens* (polychaeta). Mech Dev. 2002;115:177–9.
28. Kulakova M, Bakalenko N, Novikova E, Cook CE, Eliseeva E, Steinmetz PR, Kostyuchenko RP, Dondua A, Arendt D, Akam M, Andreeva T. Hox gene expression in larval development of the polychaetes *Nereis virens* and *Platynereis dumerilii* (Annelida, Lophotrochozoa). Dev Genes Evol. 2007;217:39–54.
29. Lee PN, Callaerts P, De Couet HG, Martindale MQ. Cephalopod Hox genes and the origin of morphological novelties. Nature. 2003;424:1061–5.
30. Lee Y, Choe J, Park OH, Kim YK. Molecular mechanisms driving mRNA degradation by m6A modification. Trends Genet. 2020;36:177–88.
31. Li Y, Nong W, Baril T, Yip HY, Swale T, Hayward A, Ferrier DK, Hui JH. Reconstruction of ancient homeobox gene linkages inferred from a new high-quality assembly of the Hong Kong oyster (*Magallana hongkongensis*) genome. BMC Genom. 2020;21:1–17.
32. Love MI, Huber W, Anders S. Moderated estimation of fold change and dispersion for RNA-seq data with DESeq2. Genome Biol. 2014;15:550.
33. Mallo M. Shaping Hox gene activity to generate morphological diversity across vertebrate phylogeny. Essays Biochem. 2022;66:717–26.
34. Mallo M, Alonso CR. The regulation of Hox gene expression during animal development. Development. 2013;140:3951–63.
35. Martin M. Cutadapt removes adapter sequences from high-throughput sequencing reads. EMBnet. 2011;17:3.
36. Martín-Durán JM, Vellutini BC, Marlétaz F, Cetrangolo V, Cvetesic N, Thiel D, Henriet S, Grau-Bové X, Carrillo-Baltodano AM, Gu W, Kerbl A, Marquez Y, Bekkouche N, Chourrout D, Gomez-Skarmeta JL, Irimia M, Lenhard B, Worsaee K, Hejnol A. Conservative route to genome compaction in a miniature annelid. Nat Ecol Evol. 2021;5:231–42.
37. Martín-Zamora FM, Liang Y, Guynes K, Carrillo-Baltodano AM, Davies BE, Donnellan RD, Tan Y, Moggioli G, Seudre O, Tran M, Mortimer K, Luscombe NM, Hejnol A, Marletaz F, Martin-Duran JM. Annelid functional genomics reveal the origins of bilaterian life cycles. Nature. 2023;615:105–10.
38. Maslakov GP, Kulishkin NS, Surkova AA, Kulakova MA. Maternal transcripts of Hox genes are found in oocytes of *Platynereis dumerilii* (Annelida, Nereididae). J Dev Biol. 2021;9:37.
39. McCain ER. Poecilogony as a tool for understanding speciation: Early development of *Streblospio benedicti* and *Streblospio gynobranchiata* (Polychaeta: Spionidae). Invertebr Reprod Dev. 2008;51:91–101.
40. Minh BQ, Nguyen MAT, Von Haeseler A. Ultrafast approximation for phylogenetic bootstrap. Mol Biol Evol. 2013;30:1188–95.
41. Modak TH, Literman R, Puritz JB, Johnson KM, Roberts EM, Proestou D, Guo X, Gomez-Chiarri M, Schwartz RS. Extensive genome-wide duplications in the eastern oyster (*Crassostrea virginica*). Philos Trans R Soc B. 2021;376:20200164.
42. Monteiro AS, Ferrier DE. Hox genes are not always Colinear. Int J Biol Sci. 2006;2:95.
43. Nguyen LT, Schmidt HA, Von Haeseler A, Minh BQ. IQ-TREE: a fast and effective stochastic algorithm for estimating maximum-likelihood phylogenies. Mol Biol Evol. 2015;32:268–74.
44. Onimaru K, Tatsumi K, Tanegashima C, Kadota M, Nishimura O, Kuraku S. Developmental hourglass and heterochronic shifts in fin and limb development. Elife. 2021;10:e62865.
45. Patro R, Duggal G, Love MI, Irizarry RA, Kingsford C. Salmon provides fast and bias-aware quantification of transcript expression. Nat Methods. 2017;14:417–9.
46. Pernet B, McArthur L. Feeding by larvae of two different developmental modes in *Streblospio benedicti* (Polychaeta: Spionidae). Mar Biol. 2006;149:803–11.
47. Peterson KJ, Irvine SQ, Cameron RA, Davidson EH. Quantitative assessment of Hox complex expression in the indirect development of the polychaete annelid *Chaetopterus* sp. Proc Natl Acad Sci USA. 2000;97:4487–92.
48. Salamanca-Díaz DA, Calcino AD, de Oliveira AL, Wanninger A. Non-collinear Hox gene expression in bivalves and the evolution of morphological novelties in mollusks. Sci Rep. 2021;11:1–12.
49. Schiemann SM, Martín-Durán JM, Børve A, Vellutini BC, Passamaneck YJ, Hejnol A. Clustered brachiopod Hox genes are not expressed collinearly and are associated with lophotrochozoan novelties. Proc Natl Acad Sci USA. 2017;114:E1913–22.
50. Seo HC, Edvardsen RB, Maeland AD, Bjordal M, Jensen MF, Hansen A, Flaat M, Weissenbach J, Lehrach H, Wincker P, Reinhard R, Chourrout D. Hox cluster disintegration with persistent anteroposterior order of expression in *Oikopleura dioica*. Nature. 2004;431:67–71.
51. Shankland M, Seaver EC. Evolution of the bilaterian body plan: What have we learned from annelids? Proc Natl Acad Sci USA. 2000;97:4434–7.

52. Skinner ME, Uzilov AV, Stein LD, Mungall CJ, Holmes IH. JBrowse: a next-generation genome browser. Genome Res. 2009;19:1630–8.
53. Wickham H. ggplot2: Elegant graphics for data analysis. Berlin: Springer; 2016.
54. Wolf JB. Cytonuclear interactions can favor the evolution of genomic imprinting. Evolution. 2009;63:1364–71.
55. Yu BD, Hess JL, Horning SE, Brown GA, Korsmeyer SJ. Altered Hox expression and segmental identity in Mll-mutant mice. Nature. 1995;378:505–8.
56. Zakas C. *Streblospio benedicti*: a genetic model for understanding the evolution of development and life-history. Curr Top Dev Biol. 2022;147:497–521.
57. Zakas C, Deutscher JM, Kay AD, Rockman MV. Decoupled maternal and zygotic genetic effects shape the evolution of development. Elife. 2018;7:e37143.
58. Zakas C, Harry ND, Scholl EH, Rockman MV. The genome of the poecilogonous annelid *Streblospio benedicti*. Genome Biol Evol. 2022;14:evac008.

Publisher's Note